EPS-0470
Submitted to Pa 4 and Pl 1,3

Measurement of the Proton Structure Function $F_2(x, Q^2)$ at HERA

H1 Collaboration

Abstract:

Preliminary results on a measurement of the proton structure function $F_2(x, Q^2)$ are reported for momentum transfers squared Q^2 between 2 GeV^2 and 5000 GeV^2 and for Bjorken x between $5 \cdot 10^{-5}$ and 0.32, using data collected by the HERA experiment H1 in 1994. The data represent an increase in statistics of a factor 10 with respect to the F_2 analysis of the 1993 data. F_2 increases significantly with decreasing x, even in the lowest reachable Q^2 region. The data are well described by a Next to leading order QCD fit.

1 Introduction

The measurement of the inclusive deep inelastic lepton-proton scattering cross section has been of great importance for the understanding of quark-gluon substructure of the proton [1]. Experiments at HERA extend the previously accessible kinematic range up to very large squared momentum transfers, $Q^2 > 5 \cdot 10^4$ GeV^2, and to very small values of Bjorken $x < 10^{-4}$. The first observation was reported of a rise of the proton structure function $F_2(x, Q^2)$ at low $x < 10^{-2}$ with decreasing x [2, 3], based on data collected in 1992. This rise was confirmed with the more precise data of 1993[4, 5]. Such a behaviour is qualitatively expected in the double leading log limit of Quantum Chromodynamics [6]. It is, however, not clarified whether the linear QCD evolution equations, as the conventional DGLAP evolution [7] in $\ln Q^2$ and/or the BFKL evolution [8] in $\ln(1/x)$, describe the rise of F_2 or whether there is a significant effect due to nonlinear parton recombination [9]. Furthermore, it is unclear whether this rise will persist at low Q^2, say of the order of a few GeV^2. For example Regge inspired models expect F_2 to be flatter for small Q^2. The quantitative investigation of the quark-gluon interaction dynamics at low x is one of the major challenges at HERA. It requires high precision for the F_2 measurement and an investigation of the hadronic final state[8].

The structure function $F_2(x, Q^2)$ is derived from the inclusive lepton-proton scattering cross section. It depends on the squared four momentum transfer Q^2 and the scaling variable x. These variables are related to the inelasticity parameter y and to the total squared centre of mass energy of the collision s as $Q^2 = xys$ with $s = 4E_eE_p$. In 1994 the incident electron energy was $E_e = 27.6$ GeV and the proton energy was $E_p = 820$ GeV. The data were recorded with the H1 detector, which is described in [10]. A salient feature of the HERA collider experiments is the possibility of measuring not only the scattered electron but also the complete hadronic final state, apart from losses near the beam pipe. This means that the kinematical variables x, y and Q^2 can be determined with complementary methods which experimentally are sensitive to different systematic effects. These methods were exploited and detailed already in [4] describing the analysis of the 1993 data. The comparison of the results obtained with different methods improves the accuracy of the F_2 measurement. A convenient combination of the results ensures maximum coverage of the available kinematic range.

In this paper an analysis is presented of inclusive deep inelastic scattering (DIS) data taken by the H1 collaboration in 1994 with an integrated luminosity of 2.2 pb^{-1}, an order of magnitude larger than in 1993. The accessible kinematic range has also been extended to the very high Q^2 region and the behaviour of F_2 has been investigated at a new level of precision.

Due to the large interest for the F_2 behaviour at small Q^2, several efforts were made to increase the acceptance for this kinematic region. For DIS events at low Q^2 the electron is scattered under a large angle θ_e (the polar angles θ are defined w.r.t the proton beam direction, termed "forward" region). Therefore the acceptance of electrons in the backward region has to be increased. This was realized as follows. i) As a result of the good accelerator background conditions, for part of the time the most inner parts of the backward electromagnetic calorimeter (BEMC) around the beampipe could be included in the trigger. Since these additional active elements are of triangular shape, these data will be reffered to as "open triangle" data sample and an integrated luminosity was accumulated of 0.27 pb^{-1} under these conditions. ii) Following a pilot excercise performed last year, we now collected 58nb^{-1} of data for which the interaction point was shifted by 62 cm, in the forward direction, leading to an average vertex position of +67 cm which results in an increase of the electron acceptance. This sample is refered to as the "shifted vertex" data sample. iii) The low Q^2 region was also covered by analyzing events which originated from the early proton satellite bunch, present during all periods of the HERA operation, which collided with an electron bunch at $z \simeq +68$ cm. These data, refered to as "satellite" data sample amount to $\simeq 3\%$ of the total data. A total "luminosity" of 68 nb^{-1} was collected over the whole run period.

The large statistics sample, taken with the nominal HERA conditions is called the "nominal vertex sample".

2 Kinematics and Event Selection

The kinematic variables of the inclusive scattering process $ep \rightarrow eX$ can be reconstructed in different ways using measured quantities from the hadronic final state and from the scattered electron. The choice of the reconstruction method for Q^2 and y determines the size of systematic errors, acceptance and radiative corrections. The basic formulae for Q^2 and y used in the different methods used are given in [4]. The methods used in the analysis of the 1994 data are: i) the so called "electron method" (E), using only the information of the scattered electron, which has the best resolutions on x and Q^2 at large y and is independent of the hadron reconstruction, apart from the vertex requirement; ii) the so called "Σ method", (Σ), calculated from the electron and hadronic final states measurements, which has small radiative corrections and extends from very low to large y values. The application of different methods was important to check that the systematic errors were correctly evaluated.

To reduce the systematic errors of the F_2 measurement, a strict data selection was performed based on the behaviour of the main detector components. The number of accepted events per luminosity was checked to be constant within statistical errors during the full data taking period.

The luminosity was determined from the measured cross section of the Bethe Heitler reaction $e^-p \rightarrow e^-p\gamma$, measuring the hard photon bremsstrahlung data only. The precision of the luminosity for the nominal vertex position data amounts to 1.5%, i.e. an improvement of a factor 3 w.r.t the analysis of the 1993 data. For the shifted vertex data the luminosity uncertainty is 4.5%. The luminosity of the satellite data sample was obtained from the measured luminosity for the shifted vertex data multiplied by the efficiency corrected event ratio in a kinematic region common to both data sets. The uncertainty of that luminosity determination was estimated to be 5%.

The events were obtained by a calorimetric trigger (energy threshold$>$ 6 GeV) not vetoed by a time-of-flight(TOF) system. The electron candidate can be detected either in the backward electromagnetic calorimeter (BEMC) covering the angular range $155° < \theta < 177°$ or in the Liquid Argon calorimeter ($\theta < 155°$). The events are then off-line selected by requiring the presence of:
- a reconstructed vertex from the tracking system within ± 30 cm of the interaction position,
- an electron candidate with an energy $E'_e > 11$ GeV, in the well contained region of the calorimeter, corresponding approximately to the θ_e cuts shown in table 1. The electron candidate has to fullfill several criterias detailed in table 1.
- some additional conditions for non ep background rejection as detailed in [4].

	low Q^2 (shifted vtx)		low Q^2 (nominal vtx)		high Q^2	
	E method	Σ method	E method	Σ method	E method	Σ method
$\theta_e/^o$	< 176	< 176	< 173	< 173	< 150	< 150
E'_e/GeV	> 11	> 11	> 11	> 11	> 11	> 11
z_{vertex}/cm	67$\pm$ 30	67$\pm$ 30	5$\pm$ 30	5$\pm$ 30	5$\pm$ 30	5$\pm$ 30
electron	$\epsilon_1 < 5$ cm	$\epsilon_1 < 5$ cm	$\epsilon_1 < 5$ cm	$\epsilon_1 < 5$ cm	$\epsilon_4 > 50\%$	$\epsilon_4 > 65\%$
identif.	$\epsilon_2 < 5$ cm	$\epsilon_2 < 5$ cm	$\epsilon_2 < 5$ cm	$\epsilon_2 < 5$ cm	$\epsilon_3 > 3\%$	$\epsilon_5 < 30$ mrad
events	9000	12000	165000	221000	6000	7000

Table 1: *Summary of event selection criteria for the shifted vertex data and the nominal vertex data at low and high Q^2. For the open triangle data sample the θ_e cut is 174°. For the electron identification several estimators were used: ϵ_1: electron cluster radius, ϵ_2: smallest distance from the closest track to the centroid of the electron cluster ϵ_3: fraction of the electron energy deposited in the first 3 radiation lengths of the calorimeter, ϵ_4: fraction of the electron energy deposited in the 4 hottest cells of the cluster, ϵ_5: angular distance between the electron cluster and the associated track.*

The $x - Q^2$ distribution of the selected events is shown in fig.1, where the kinematical regions of the different data samples are indicated.

At low Q^2 the main sources of non-ep background are due to proton beam interactions with residual gas and beam line elements upstream of the H1 detector. An efficient reduction of the remaining background is provided by the minimum energy and the vertex requirements discussed above. The residual background was estimated to represent less than 1% of the total number of selected events. At high Q^2 the main background is due to cosmic ray events and muons travelling off axis parallel to the proton beam. Requiring a reconstructed vertex rejects most of them. The remaining background was estimated to be smaller than 1%.

The only significant background to DIS from ep interactions is due to photoproduction events at $Q^2 \simeq 0$ where the scattered electron escapes the detector along the beam pipe but in which an energy cluster from the hadronic final state fakes an electron. About 10% of these events are identified as photoproduction background if the scattered electron is found in the electron tagger. To estimate this background, photoproduction events were simulated corresponding to the luminosity of the data. The photoproduction background was subtracted statistically bin by bin, where only 12 bins, out of a total of 172 (x, Q^2) bins have a contamination larger than 3%. This contamination never exceeds 15% in any bin.

More than one million Monte Carlo DIS events were generated using DJANGO [11] and different quark distribution parametrizations, corresponding to an integrated luminosity of approximately 20 pb^{-1}. The program is based on HERACLES [12] for the electroweak interaction and on LEPTO [13] to simulate the hadronic final state. HERACLES includes first order radiative corrections, the simulation of real bremsstrahlung photons and the longitudinal structure function. The acceptance corrections were performed using the GRV parametrization [14], which describes rather well the HERA F_2 results of 1993 for $Q^2 > 10$ GeV^2. LEPTO uses the colour dipole model (CDM) as implemented in ARIADNE [15] which is in good agreement with data on the energy flow and other characteristics of the final state as measured by H1 [16] and ZEUS [17]. For the estimation of systematic errors connected with the topology of the hadronic final state, the HERWIG model [18] was used in a dedicated analysis. Based on the GEANT program [19] the detector response was simulated in detail.

After this step the Monte Carlo events were subject to the same reconstruction and analysis chain as the real data.

3 Structure Function Measurement

The structure function $F_2(x, Q^2)$ was derived after radiative corrections from the one-photon exchange cross section

$$\frac{d^2\sigma}{dxdQ^2} = \frac{2\pi\alpha^2}{Q^4x}(2 - 2y + \frac{y^2}{1+R})F_2(x, Q^2) \tag{1}$$

Effects due to Z boson exchange are smaller than 2%. The structure function ratio $R = F_2/2xF_1 - 1$ has not been measured yet at HERA and was calculated using the QCD relation [20] and the GRV structure function parametrization. Compared to the previous H1 analysis [4] the F_2 measurement has been extended to lower and higher Q^2 (from $4.5-1600$ GeV^2 to $2-5000$ GeV^2), and to lower and higher x (from $1.8\cdot10^{-4}-0.13$ to $5\cdot10^{-5}-0.32$). The determination of the structure function requires the measured event numbers to be converted to the bin averaged cross section based on the Monte Carlo acceptance calculation. All detector efficiencies were determined from the data utilizing the redundancy of the apparatus. Apart from very small extra corrections all efficiencies are correctly reproduced by the Monte Carlo simulation. The bin averaged cross section was corrected for higher order QED radiative contributions and a bin size correction was performed. This determined the one-photon exchange cross section which according to eq.1 led to the values for $F_2(x, Q^2)$.

Due to the different data sets available: nominal vertex data, "open triangle" data , "shifted vertex" data and "satellite data", which have different acceptances and use for a given Q^2, x point different parts of the detectors, cross checks could be made in kinematic regions of overlap. The results were found to be in very good agreement with each other for both kinematic reconstruction methods (E and Σ).

To increase the significance, the results of the shifted vertex data sample and satellite data sample, which have about the same number of events, were combined in those bins where satellite data was available ($3.5 \leq Q^2 \leq 6.5$ GeV^2). The extra luminosity uncertainty for the satellite data (5%) was added to the statistical error of those data. The correlations between the systematic errors were taken into account for the error calculation. In this paper data are presented from the shifted vertex analysis alone ($Q^2 \leq 3.5$ GeV^2), from a combination of the shifted vertex and satellite analysis ($3.5 < Q^2 \leq 6.5$ GeV^2), from the open triangle analysis ($Q^2 = 8.5$ GeV^2) and from the nominal high statistics sample ($Q^2 > 8.5$GeV^2)

The large available statistics allows to make very detailed studies on the detector response: efficiencies and calibration. As a result the systematic errors on many effects are reduced, compared to the analysis presented in[4]. A list of the systematics errors with preliminary, conservative values is given below.

- A potential miscalibration of the electron energy by 1.5% in the BEMC, and by 2-3% in the Liquid Argon calorimeter

- A 5% scale error for the hadronic energy in the LAr calorimeter, the effect of which is reduced due to the joint consideration of tracks and calorimeter cells for the Σ analysis. A 20% scale error was assigned to the energy of the hadronic final state measured in the BEMC. These numbers include uncertainties due to the noise treatment for the LAr calorimeter and the BEMC.

- A shift of up to 1 mrad for the electron polar angle. Errors of the energy and angular resolutions are taken into account in addition to possible shifts of mean values.

- Apart from the electron identification all efficiencies were determined from the data and compared with the Monte Carlo simulation. Agreement between the experimental and the simulated values for the individual efficiencies was found to be better than 2%. An overall error of 4% was assigned due to the imperfect description of the various efficiencies. A larger error of at most $5-8\%$ was added to account for the vertex reconstruction efficiency variation at large x.

- An error of up to 3% in the radiative correction due to uncertainties from the hadronic corrections, the cross section extrapolation towards $Q^2 = 0$, second order corrections and the absence of the soft photon exponentiation in the HERACLES Monte Carlo. The accuracy was cross checked by comparing the Monte Carlo estimate with TERAD [21]. A direct estimate has been made comparing in their overlap region the cross sections derived from the E and the Σ methods.

- The structure function dependence of the acceptance and bin size corrections which was controlled to better than 2%. The comparison of the different simulation models of the hadronic final state mentioned above was used to assign an additional 2% systematic error to the hadronic methods.

- The uncertainty due to photoproduction background was assumed to be smaller than 30% of the correction applied, i.e. smaller than 5%. This affects only the highest y bins at lower Q^2. In particular in the new low Q^2 region this effect was studied in detail with different Monte Carlos and from the data.

- Statistical errors in the Monte Carlo acceptance and efficiency calculations were computed and added quadratically to the systematic error. Due to the very large statistics this error is small, about 3% for the shifted vertex data region and smaller elsewhere.

These systematic uncertainties affect differently the F_2 measurement done with different methods. In fig.2 the comparison of the measurement done with the E and with the Σ method is shown. Both display the rise at low x already observed in 1992 and 1993 [2, 4] above 8.5 GeV^2, and are in good agreement for all Q^2 values, indicating a correct estimation of the systematic errors. With the 1994 data, we can observe that the strong rise at low x remains down to the lowest x and Q^2 values reached in this analysis.

The two measurements are combined using the E method for $y > 0.15$ and the Σ method for $y < 0.15$. The result is shown in fig.3. The measurements have a typical (preliminary) systematic error of 10%, and are based on roughly 10 times the statistics of the 1993 data. Apart from the new domain reached at low Q^2, the large amount of data collected in 1994 allows for the measurement of F_2 for Q^2 values up to 5000 GeV^2, and to achieve a statistical precision between 8.5 and 65 GeV^2 of the order of 2%. The results are in good agreement with the previous H1 publication [4] concerning the shape, but are about 5% lower in absolute normalization. Note that the luminosity uncertainty for the 1993 data was 4.5%, while now this has been improved to the level of 1.5%.

In fig.3, the H1 data shows that the steep rise of F_2 at low x persists in the new domain explored, i.e. down to $Q^2 = 2$ GeV^2 and $x = 5 \cdot 10^{-5}$, and that the "slope" of this rise increases with Q^2, as expected from perturbative QCD. The data of fixed target muon-proton experiments are added as well, showing the smooth transition from these to the HERA data at larger Q^2 values and emphasising the rise of the F_2 with decreasing x for Q^2 values below 10 GeV^2.

The result of a Next-to-Leading Order (NLO) QCD fit performed as explained in [23] on the data with $Q^2 \geq 5$ GeV^2 is also shown in the fig.3. The F_2 behaviour can be well described by the DGLAP evolution equations within the present preliminary errors. The data for Q^2 values below 5 GeV^2 are also compatible with the extrapolation of the fit in this region, as can be seen in the figure.

In Fig.4 we show the 7 lowest Q^2 bins from this analysis, together with an F_2 measurement at lower Q^2, extracted from the analysis of the radiative DIS events in the same data sample. The latter is detailed in [24]. From this analysis 3 points are also added in the 2.5 GeV^2 bin, at the high x end. The data are compared to current model predictions and extrapolations from fits to data. The Regge inspired models DOLA[26] and CKMT[25] generally undershoot the data, while the GRV parametrization gives a good description of the data. At higher Q^2 the MRS[28] and CTEQ[27] distributions are in accord with the data.

The persistent rise of F_2 at low x, when going down in Q^2 indicates that the photoproduction regime has not been reached yet. This can also be seen in fig. 5 which shows for the low Q^2 data the strong rise of F_2 as a function of W, the invariant mass of the $\gamma^* p$ system (at low x, $W \simeq \sqrt{Q^2/x}$). F_2 is related to the total cross-section of the proton-virtual photon interaction ($\sigma_{tot}(\gamma^* p)$) via

$$\sigma_{tot}(\gamma^* p) \simeq \frac{4\ \pi^2 \alpha}{Q^2} F_2(W, Q^2). \tag{2}$$

The F_2 growth can be contrasted with the weak rise with W of the total real photoproduction cross-section in the same range of W : 20-225 GeV [30, 31].

Fig.6 shows the dependence of F_2 on Q^2 at fixed x. The violation of scaling appears to be stronger for smaller values of x, a trend already observed in fixed target experiments for $x \leq 0.1$. This behaviour is now clearly visible for x below $2 \cdot 10^{-4}$. The curve shows the result of the NLO QCD fit. The gap visible around 100 GeV^2 corresponds to a boundary region between two calorimeters in the H1 detector, for which the F_2 analysis is still in progress.

Based on earlier QCD studies [23] Ball and Forte [32] show that evolving a flat input distribution at some Q_0, of the order of 1 GeV^2, with the DGLAP equations leads to a strong rise of F_2 at low x in the region measured by HERA. An interesting feature is that if QCD evolution is the underlying dynamics of the rise, perturbative QCD predicts that at large Q^2 and small x the structure function exhibits double scaling in the two variables:

$$\sigma \equiv \sqrt{\log(x_0/x) \cdot \log(t/t_0)}, \quad \rho \equiv \sqrt{\frac{\log(x_0/x)}{\log(t/t_0)}} \tag{3}$$

with $t \equiv \log(Q^2/\Lambda^2)$.

In order to test this prediction H1 data are presented in the variables σ and ρ, taking the boundary conditions to be $x_0 = 0.1$ and $Q_0^2 = 0.5$ GeV^2, and $\Lambda_{\rm LO}^{(4)} = 185$ MeV. In a previous analysis [29] we chose $Q_0^2 = 1$ GeV^2, but the new low Q^2 data clearly indicate that F_2 is not yet flat for this Q^2 value.

The measured values of F_2 are rescaled by

$$R'_F(\sigma, \rho) = 8.1 \ \exp\left(\delta \frac{\sigma}{\rho} + \frac{1}{2}\log(\sigma) + \log(\frac{\rho}{\gamma})\right), \tag{4}$$

to remove the part of the leading subasymptotic behaviour which can be calculated in a model independent way; $\log(R'_F F_2)$ is then predicted to rise linearly with σ. Scaling in ρ can be shown by multiplying F_2 by the factor $R_F \equiv R'_F e^{-2\gamma\sigma}$. Here $\gamma \equiv 2\sqrt{3/b_0}$ with b_0 being the leading order coefficient of the β function of the QCD renormalization group equation for four flavours, $\delta = 1.36$ for four flavours and three colours.

Fig. 7a shows $R_F F_2$ versus ρ. Scaling roughly sets in for $\rho \geq 1.5$. Fig. 7b, for $\rho \geq 1.5$, shows nice scaling behaviour, namely a linear of $\log(R'_F F_2)$ with σ.

4 Summary

A measurement has been presented of the proton structure function $F_2(x, Q^2)$ in deep inelastic electron-proton scattering at HERA with data taken in the running period of 1994. The integrated luminosity is 2.2 pb^{-1} which represents a tenfold increase in statistics compared to the H1 F_2 analysis based on the 1993 data. The structure function measurement includes data from different detector components and running configurations. Low Q^2 values are reached using data with the ep interaction vertex shifted from the nominal position. The data cover a kinematic range for Q^2 between 2 and 5000 GeV^2 and x between $5.0 \cdot 10^{-5}$ and 0.32.

The F_2 values presented are obtained using different methods to reconstruct the inclusive scattering kinematics. At high values of the scaling variable $y \geq 0.15$, due to its superior resolution, the electron method is used which is based on the scattered electron energy and angle. Lower y values are covered with the Σ method which combines electron and hadronic information to reduce radiative corrections and calibration errors. The data show a smooth transition from the fixed target high x data to the HERA low x data.

A distinct rise of the structure function with decreasing x at fixed Q^2 is confirmed. Around $x \sim 10^{-3}$ the decrease of x by an order of magnitude amounts to a rise of F_2 of about a factor two. The rise is persistent at small Q^2 values, down to 2 GeV^2. The data can be described by a NLO QCD fit. Double asymptotic scaling still holds, when a Q_0^2 scale smaller than 1 GeV^2 is used.

Acknowledgements

We are very grateful to the HERA machine group whose outstanding efforts made this experiment possible. We acknowledge the support of the DESY technical staff. We appreciate the big effort of the engineers and technicians who constructed and maintained the detector. We thank the funding agencies for financial support of this experiment. We wish to thank the DESY directorate for the support and hospitality extended to the non-DESY members of the collaboration.

References

[1] for a recent review see: J. Feltesse, DAPNIA-SPP-94-35(1994), Invited talk at the 27. International Conference on High Energy Physics, Glasgow, Scotland, 1994.

[2] H1 Collab., I. Abt et al., Nucl. Phys. **B407** (1993) 515.

[3] ZEUS Collab., M. Derrick et al., Phys. Lett. **B316** (1993) 412.

[4] H1 Collab., T. Ahmed et al., Nucl. Phys. **B439** (1995) 471.

[5] ZEUS Collab., M. Derrick et al., Z. Phys. **C65** (1995), 379.

[6] A. De Rújula et al, Phys. Rev. **D10** (1974) 1649.

[7] Yu. L. Dokshitzer, Sov. Phys. JETP **46** (1977) 641;
V. N. Gribov and L.N. Lipatov, Sov. J. Nucl. Phys. **15** (1972) 438 and 675;
G. Altarelli and G. Parisi, Nucl. Phys. **B126** (1977) 297.

[8] H1 Collab, S. Aid et al, DESY preprint 95-108 (1995)

[9] L. V. Gribov, E. M. Levin and M. G. Ryskin, Phys. Rep. **100** (1983) 1;
A. H. Mueller and N. Quiu, Nucl. Phys. **B268** (1986) 427.

[10] H1 Collab., I. Abt et al., DESY 93-103 (1993).

[11] G. A. Schuler and H. Spiesberger, Proceedings of the Workshop Physics at HERA, vol. 3, eds. W. Buchmüller, G. Ingelman, DESY (1992) 1419.

[12] A. Kwiatkowski, H. Spiesberger and H.-J. Möhring, Computer Phys. Comm. **69** (1992) 155.

[13] G. Ingelman, Proceedings of the Workshop Physics at HERA, vol. 3, eds. W. Buchmüller, G. Ingelman, DESY (1992) 1366.

[14] A. D. Martin, W. J. Stirling and R. G. Roberts, Proceedings of the Workshop on Quantum Field Theory Theoretical Aspects of High Energy Physics, eds. B. Geyer and E. M. Ilgenfritz (1993) 11.

[15] L. Lönnblad, Computer Phys. Comm. **71** (1992) 15.

[16] H1 Collab., I. Abt et al., Z. Phys. **C63** (1994) 377.

[17] ZEUS Collab., M. Derrick et al., Z. Phys. **C59** (1993), 231.

[18] G. Marchesini et al., Computer Phys. Comm. **67** (1992) 465.

[19] R. Brun et al., GEANT3 User's Guide, CERN–DD/EE 84–1, Geneva (1987)

[20] G. Altarelli and G. Martinelli, Phys. Lett. **B76** (1978) 89.

[21] A. Akhundov et al., DESY 94-115 (1994).

[22] J. Blümlein, Proceedings of the Workshop Physics at HERA, vol. 3, eds. W. Buchmüller, G. Ingelman, DESY (1992) p.1270 and DESY 94-044, Z. Phys. **C** (1994) in press.

[23] H1 Collab., S. Aid et al., DESY 95-081 (1995) submitted to Phys. Lett..

[24] H1 Collab., contributed paper to 1995 EPS conference, Bruessel, eps 472.

[25] A. Capella et al., Phys. Lett. **B337** (1994) 358.

[26] A. Donnachie and P. V. Landshoff, Z. Phys. **C61** (1994) 139.

[27] CTEQ collaboration, J. Botts et al. : Phys. Lett. 304B (1993) 15
CTEQ collaboration, J. Botts et al. (to be published)

[28] A.D. Martin, W.J. Stirling and R.G. Roberts, RAL preprint RAL-95-021 (1995).

[29] H1 Collab., S. Aid et al., DESY preprint 95-081 (1995).

[30] H1 Collab., T. Ahmed et al., Phys. Lett. **B299** (1993) 374;
M. Erdmann et al., DESY 93-077 (1993);

[31] ZEUS Collab., M. Derrick et al., Phys. Lett. **B293** (1992) 465,
DESY 94-032 (1994), to be published in Z. Phys. **C**.

[32] R.D. Ball, S. Forte, Phys. Lett. **B335** (1994) 77.

[33] R.D. Ball, S. Forte, Phys. Lett. **B336** (1994) 77.

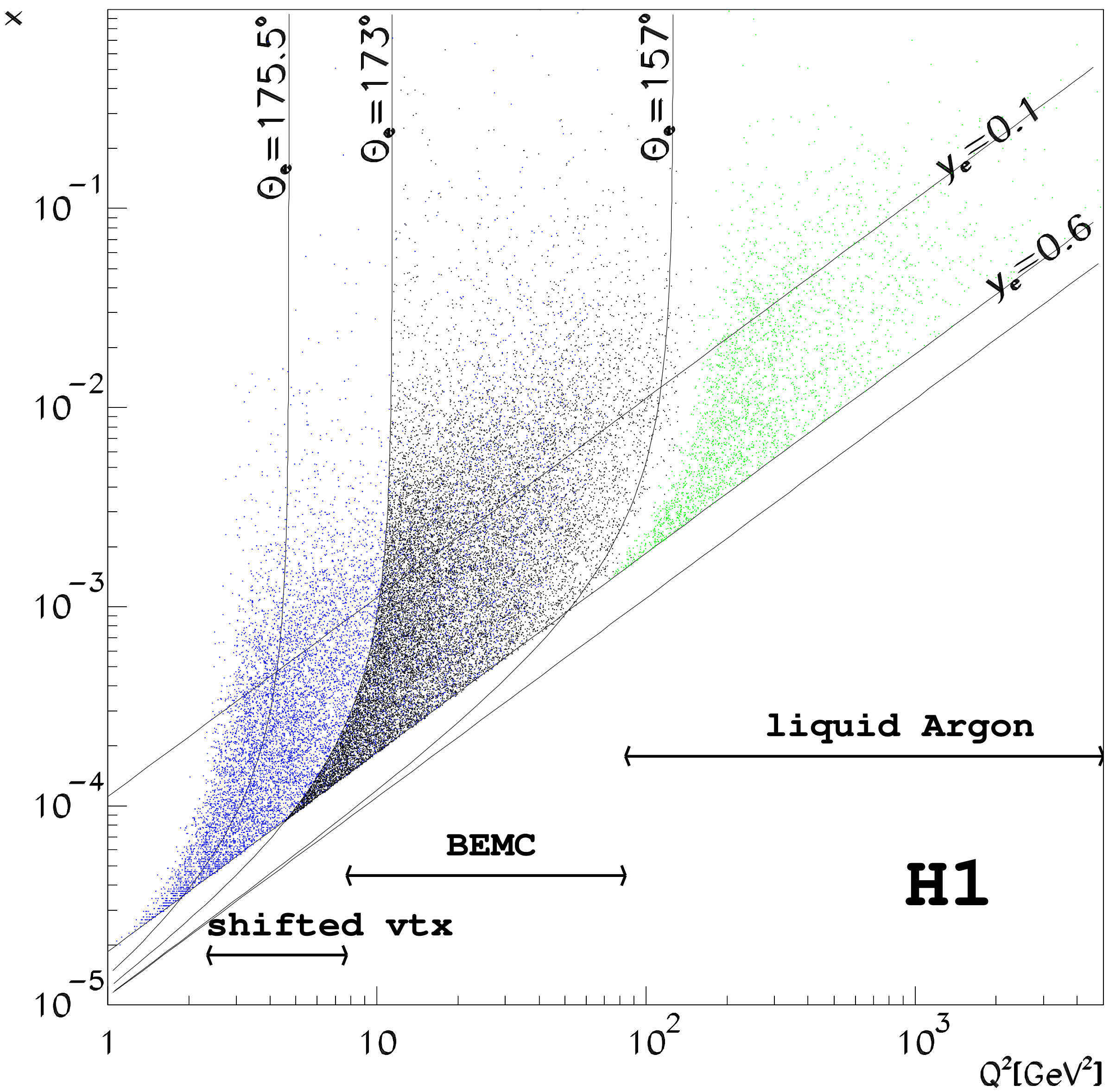

Figure 1: *Distribution of the neutral current event sample in the $x-Q^2$ plane. The acceptance for scattered electrons in the BEMC and the Liquid Argon Calorimeters are indicated. The extension of the kinematic region by shifting the vertex by 62 cm is also shown.*

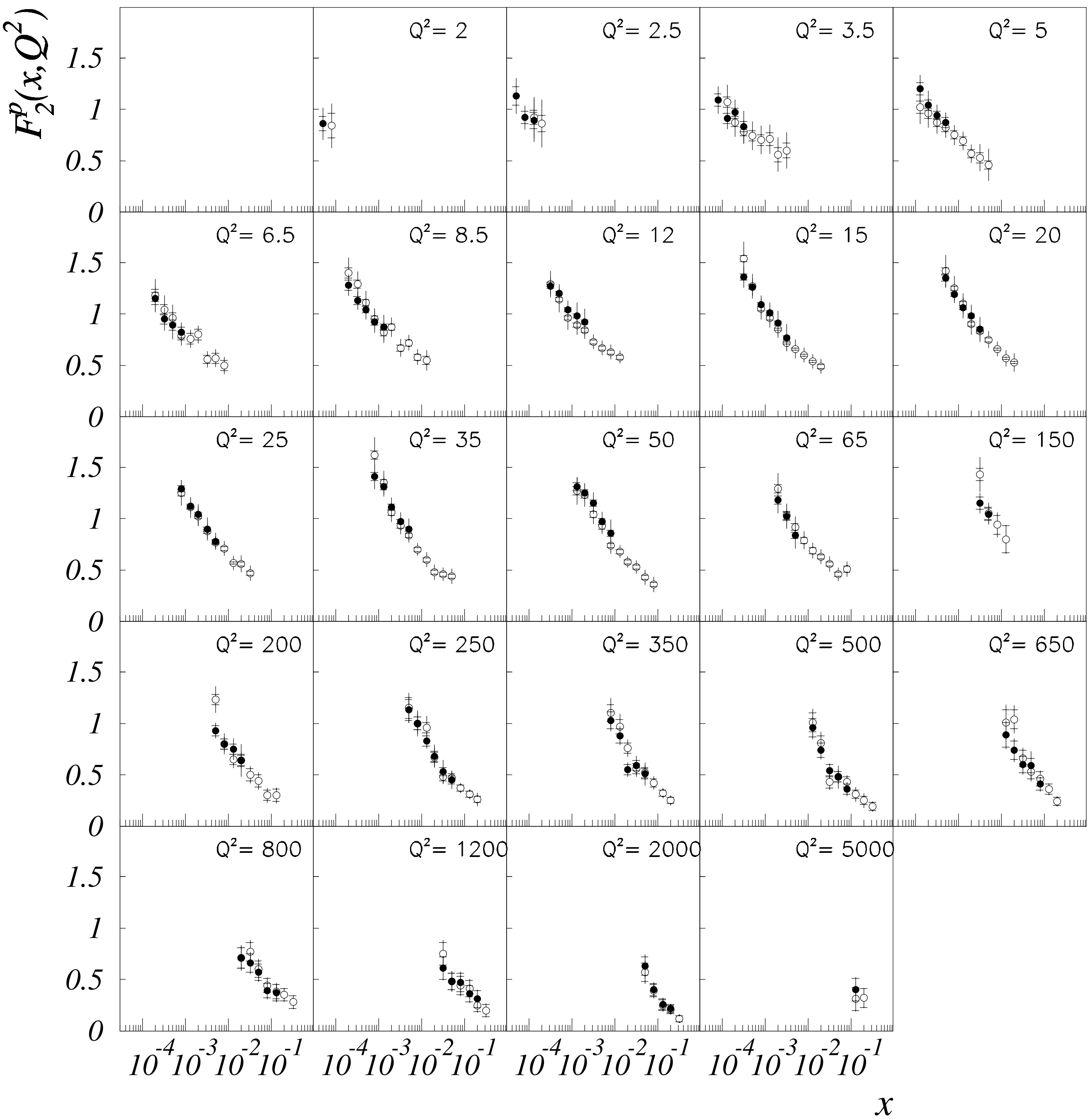

Figure 2: *Comparison of the proton structure function $F_2(x, Q^2)$ (preliminary) as function of x in different bins of Q^2 measured with the E method (full points) and with the Σ method (open points). The full error represents the statistical and systematic errors added in quadrature not taking into account the 1.5% systematic error on the luminosity measurement (4.5% for $Q^2 \leq 6.5$ GeV^2).*

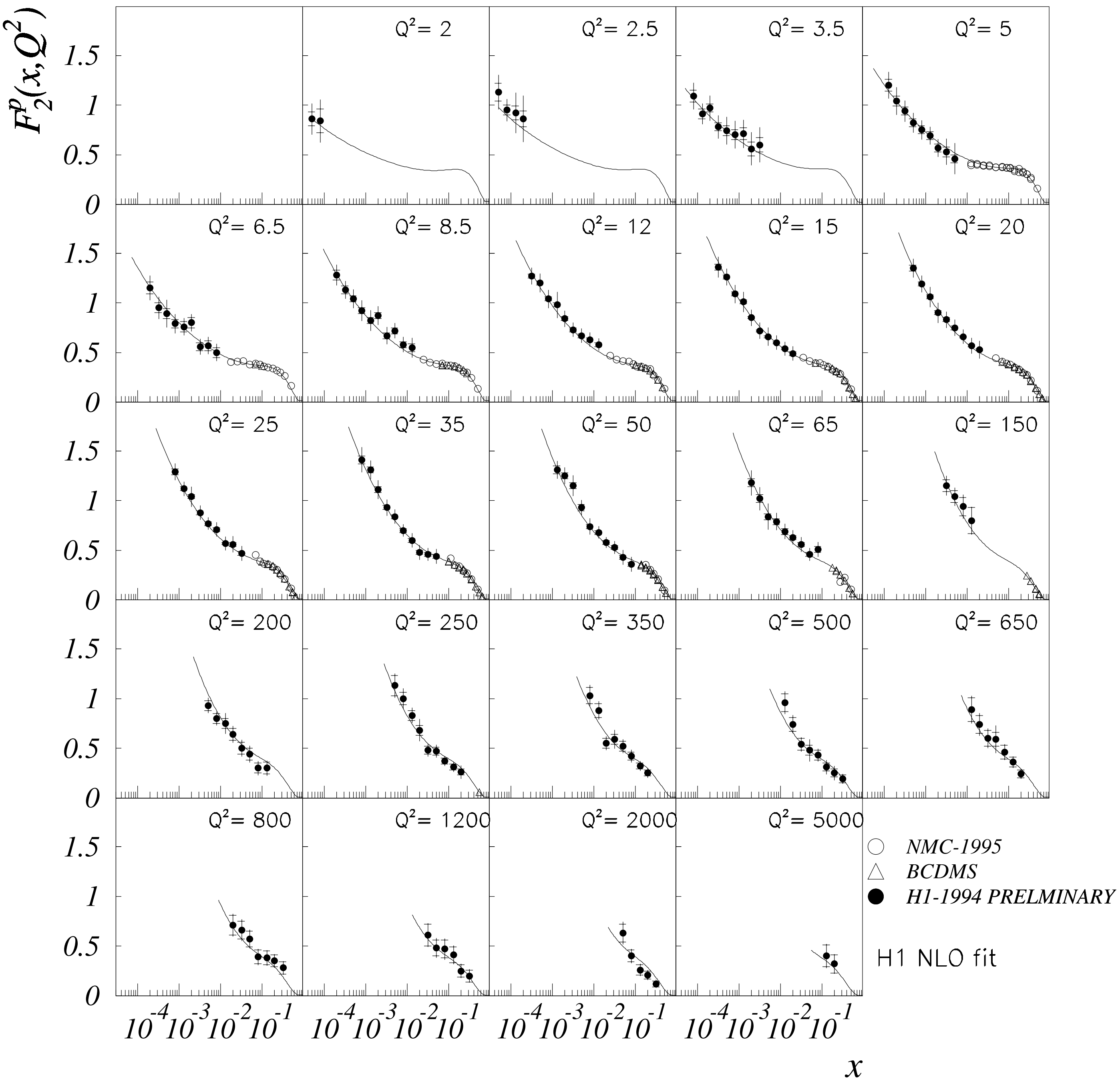

Figure 3: *Preliminary measurement of the proton structure function $F_2(x, Q^2)$ as function of x in different bins of Q^2. The inner error bar is the statistical error. The full error represents the statistical and systematic errors added in quadrature not taking into account the 1.5% systematic error on the luminosity measurement (4.5% for $Q^2 \leq 6.5$ GeV^2). Open circles and triangles represent NMC and BCDMS measurements, respectively. A smooth transition becomes apparent from the NMC and BCDMS data (open circles and triangles, respectively) to the H1 data. The curves represent a QCD fit to all data, see text.*

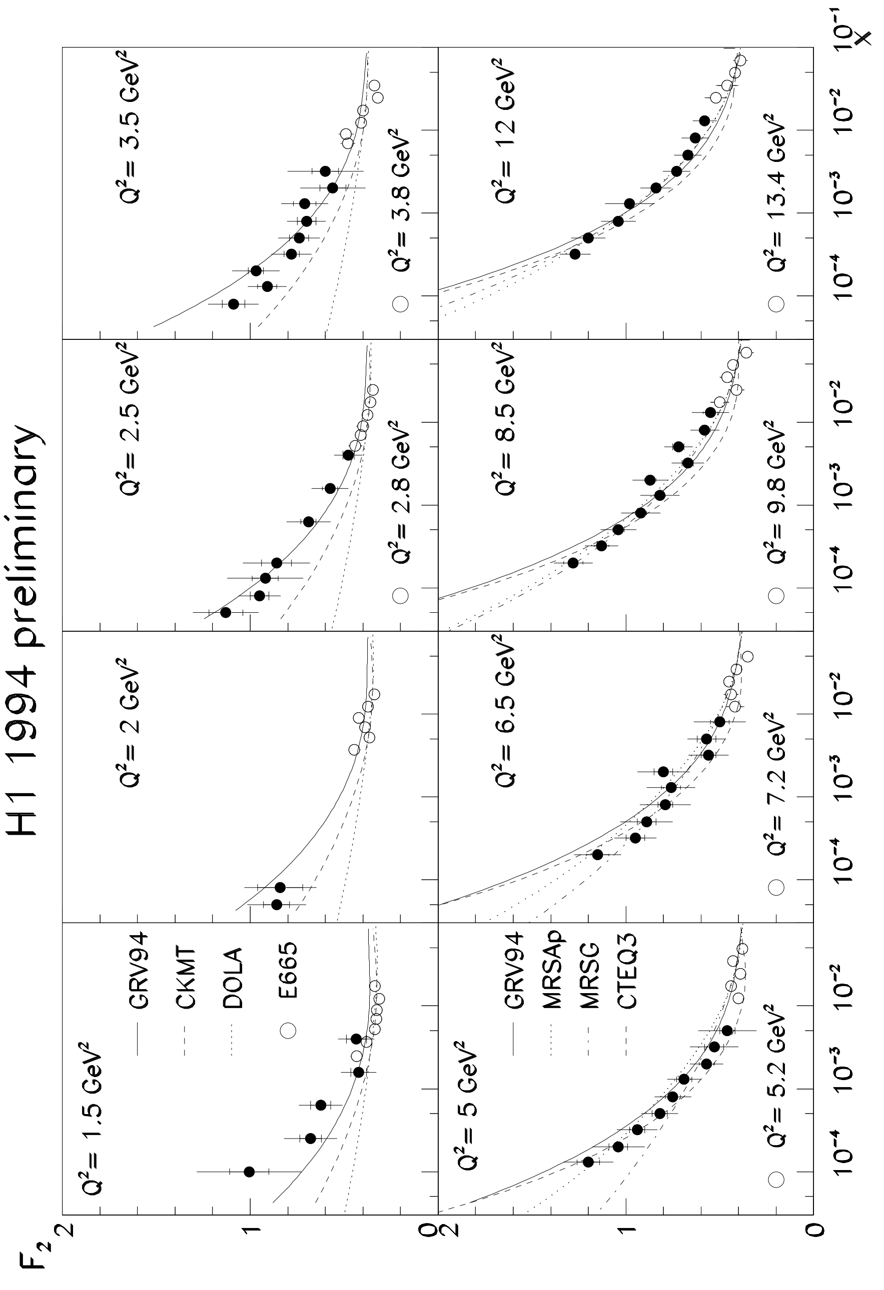

Figure 4: *Preliminary measurement of the proton structure function $F_2(x, Q^2)$ in the low Q^2 region by H1 (closed points), together with results from the E665 experiment (open points). Additionally to the data discussed in this paper, the points of the F_2 calculated with radiative events, as discussed in [24] are shown: these consist of the full bin at $Q^2 = 1.5$ GeV^2 and the 3 highest x points in the bin $Q^2 = 2.5$ GeV^2. Different predictions for F_2 are compared to the data. The DOLA and CKMT curves are only shown for the upper row of Q^2 bins; CTEQ3M, MRSG and MRSA' are shown for the lower row; GRV is shown for the full range.*

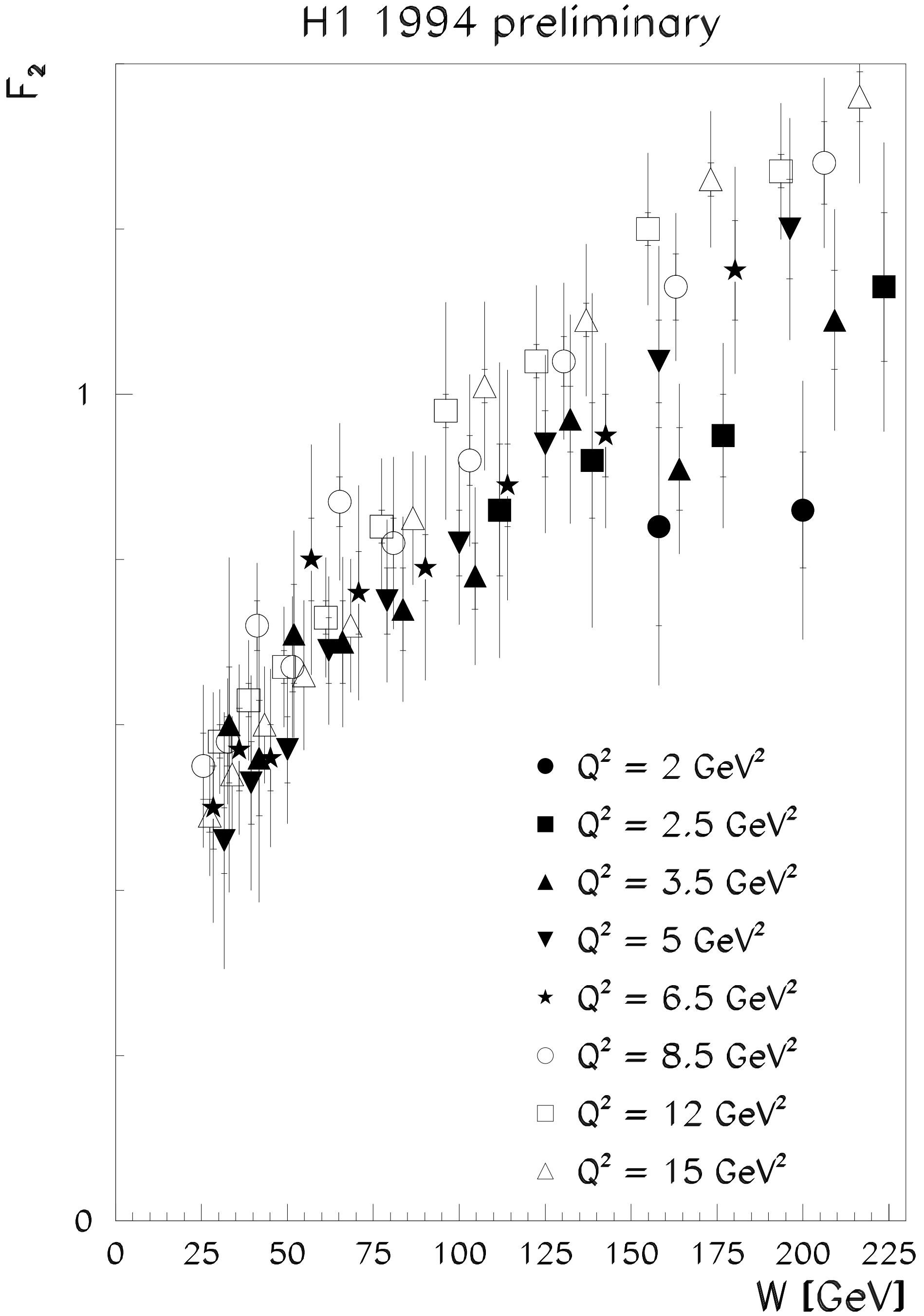

Figure 5: *Preliminary measurement of the proton structure function $F_2(W, Q^2)$ as function of W in the low Q^2 bins. The inner error bar is the statistical error. The full error represents the statistical and systematic errors added in quadrature not taking into account the 1.5% systematic error on the luminosity measurement. The strong rise of F_2 with W, indicates a different behaviour between $\sigma_{tot}(\gamma^* p)$ and $\sigma_{tot}(\gamma p)$ even at the lowest Q^2 reached in this analysis.*

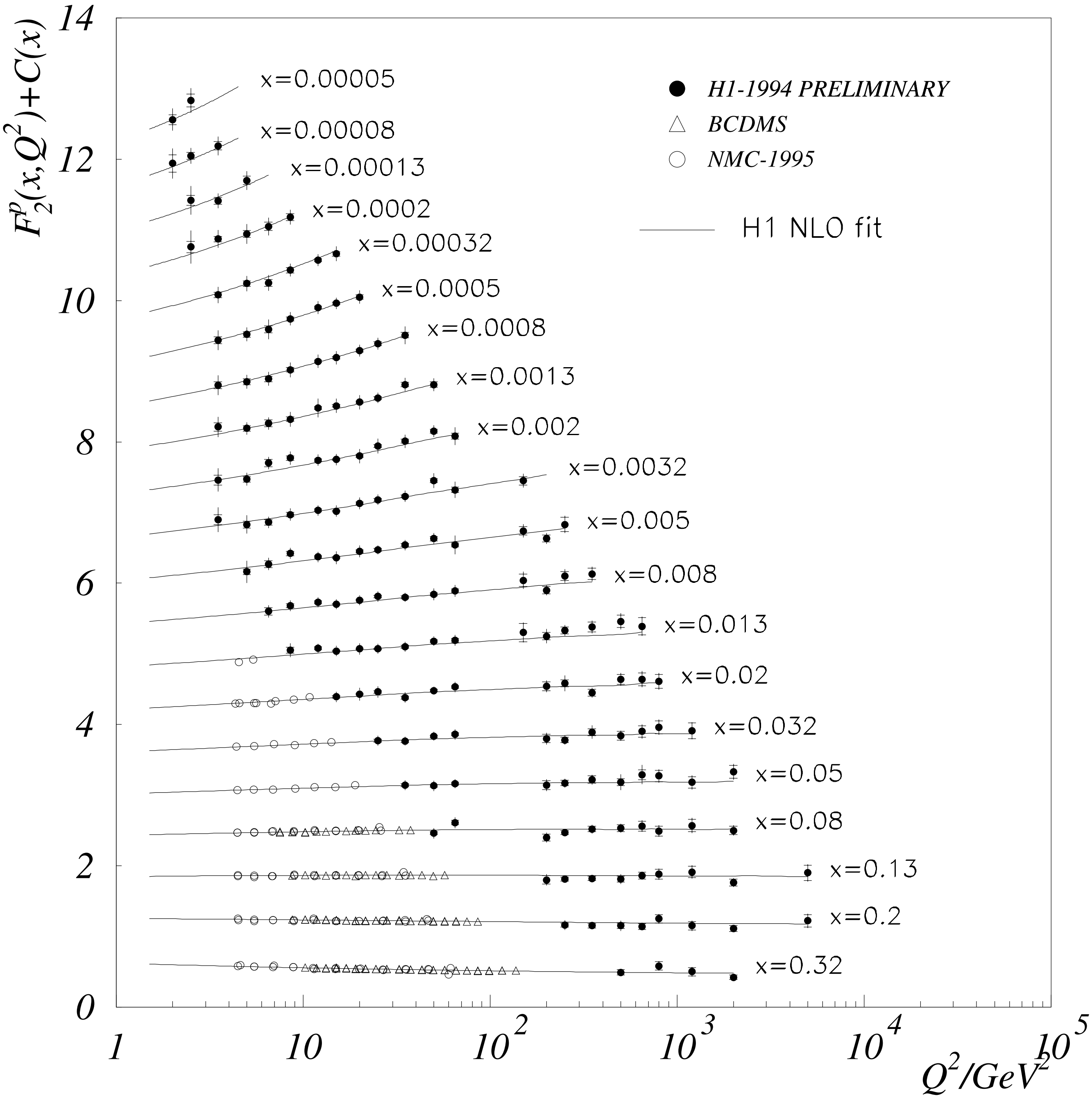

Figure 6: *Preliminary Measurement of the proton structure function $F_2(x,Q^2)$. The H1 data (closed points) is consistent with the fixed target experiments BCDMS (open triangles) and NMC (open circles). The gap visible around 100 GeV^2 corresponds to a boundary region between two calorimeters in the H1 detector, which is not completely analyzed yet. The curve represents the NLO QCD fit described in the text. The F_2 values are plotted with all but normalization errors in a linear scale adding a term $c(x) = 0.6(i_x - 0.5)$ to F_2 where i_x is the bin number starting at $i_x = 1$ for $x = 0.32$.*

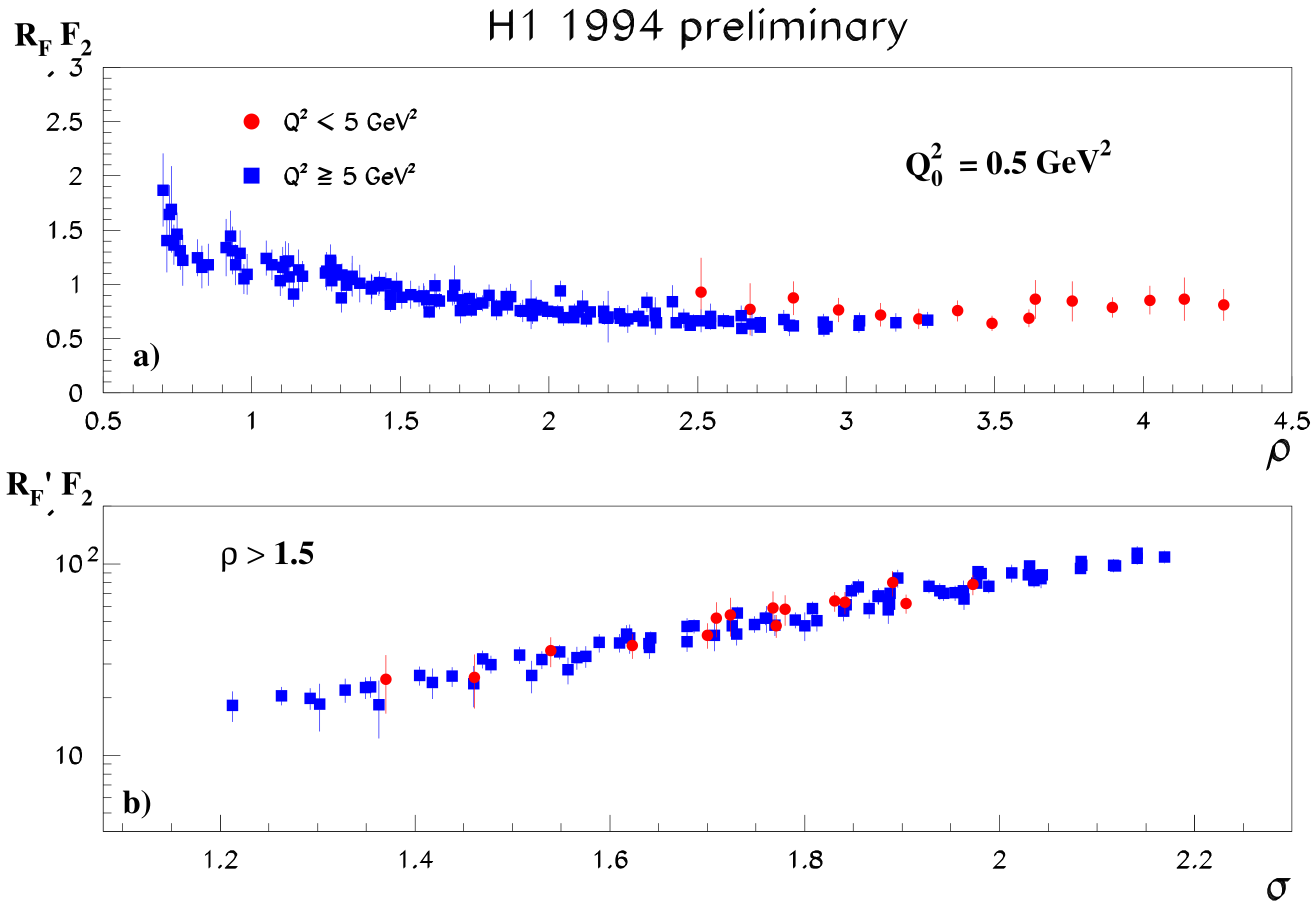

Figure 7: *The rescaled structure functions $R_F F_2$ and $R_F' F_2$ (preliminary) plotted versus the variables ρ and σ defined in the text. Only data with $\rho > 1.5$ are shown in b.*